ROYAL SOCIETY
OF CHEMISTRY

www.rsc.org/foodfunction

Rutin inhibits amylin-induced neurocytotoxicity and oxidative stress

Xiao-Lin Yu [a,1], Ya-Nan Li [b,1], He Zhang [c], Ya-Jing Su [d], Wei-Wei Zhou [a], Zi-Ping Zhang [b], Shao-Wei Wang [a], Peng-Xin Xu [a,b], Yu-Jiong Wang [**,b] , Rui-Tian Liu [*,a]

[a] *National Key Laboratory of Biochemical Engineering, Institute of Process Engineering, Chinese Academy of Sciences, Beijing 100190, China. E-mail: rtliu@ ipe.ac.cn; Fax: +86-10-82545075; Tel: +86-10-82545017*

[b] *School of Life Science, Ningxia University, Yinchuan 750021, China. E-mail: wyj@nxu.edu.cn; Fax: +86-951-2062129; Tel: +86- 951-2012033*

[c] *Department of Pharmacy, Xuanwu Hospital, Capital Medical University, Beijing 100053, China*

[d] *General Hospital of Ningxia Medical University, Yinchuan 750004, China*

[1] These authors equally contributed to this work.

Abbreviations: AD, Alzherimer's disease; Aβ, β-amyloid; T2DM, type 2 diabetes mellitus; ThT, thioflavin T; TEM, transmission electron microscope; DCFH-DA, 2',7'-dichlorfluorescein-diacetate; MTT, 3-[4,5-dimethylthiazol-2-yl]-2,5-diphenyltetrazolium bromide; ROS, reactive oxygen species; GSH, glutathione; GSSG, glutathione disulfide; MDA, malondialdehyde; SOD, superoxide dismutase; CAT, catalase; GPx, glutathione peroxidase; iNOS, inducible nitric oxide synthase; NO, nitric oxide; TNF-α, tumor necrosis factor alpha; IL-1β, interleukin 1β

ABSTRACT

Recent evidences showed that amylin deposition are not only found in pancreas in type 2 diabetes mellitus (T2DM) patients, but also in other peripheral organs, such as kidneys, heart and brain. Circling amylin oligomers that cross the blood-brain barrier and accumulate in the brain may be an important contributor to diabetic cerebral injury and neurodegeneration. Moreover, increasing epidemiological studies indicate that there is significant association between T2DM and Alzheimer's disease (AD). Amylin and β-amyloid (Aβ) may share common pathophysiology and show strikingly similar neurotoxicity profiles in the brain. To explore the potential effects of rutin on AD, we here investigated the effect of rutin on amylin aggregation by Thioflavin T dyeing, evaluated the effect of rutin on amylin-induced neurocytotoxicity by MTT assay, and assessed oxidative stress, as well as the generation of nitric oxide (NO) and pro-inflammatory cytokines in neuronal cells. Our results showed that flavonoid antioxidant rutin inhibited amylin-induced neurocytotoxicity, decreased the production of reactive oxygen species (ROS), NO, glutathione disulfide (GSSG), malondialdehyde (MDA) and pro-inflammatory cytokines TNF-α and IL-1β, attenuated mitochondrial damage and increased the GSH/GSSG ratio. These protective effects of rutin may have resulted from its ability to inhibit amylin aggregation, enhance the antioxidant enzyme activity of superoxide dismutase (SOD), catalase (CAT), and glutathione peroxidase (GPx) and reduce inducible nitric oxide synthase (iNOS) activity. These *in vitro* results indicate that rutin is a promising natural product to protect neuronal cells from amylin-induced neurotoxicity and oxidative stress, and rutin administration could be a feasible therapeutic strategy to prevent AD development and protect the aging brain or slow neurodegenerative processes.

Introduction

Amyloid deposition is a pathophysiological hallmark of some severe degenerative disorders, including Alzheimer's disease (AD), Parkinson's disease, Huntington's disease, and type 2 diabetes mellitus (T2DM)[1-4]. In T2DM, the aggregation of the human islet amyloid polypeptide (IAPP, amylin) forms islet amyloid deposits that are toxic to insulin-producing β-cells and can cause cell death[5, 6]. Human amylin is a 37-residue peptide hormone co-secreted with insulin by pancreatic β-cells[7-9]. In physiological state, human amylin in soluble monomer facilitates the effects of insulin by participating in carbohydrate metabolism and satiety[10]. However, in disease state amylin undergoes a multistep misfolding process in which the monomers are self-assembled into β-sheet-rich oligomers that ultimately form fibrils. It is believed that small, dynamic, transient, and heterogeneous amylin oligomers cause β-cell dysfunction and death by disrupting cell membrane integrity and other cell signal transduction pathways [11], whereas monomers and mature fibrils may be less toxic to β-cells [12, 13].

Amylin deposition have been detected in pancreas islets of over 95% of patients with T2DM[14, 15]. Besides pancreas, recent evidences revealed that amylin accumulation are also found in other peripheral organs, including brain [16]. Numerous epidemiological studies have shown positive correlation between T2DM and AD [17]. Patients with T2DM are at 2- to 5-times higher risk of developing AD [18, 19]. In the brain of AD patients, amylin is found to form independent amyloid plaques or co-precipitating with β-amyloid (Aβ) to form complex amylin/Aβ plaques, which inducing failure of elimination of Aβ from the brain [16]. These findings suggest that amylin may be a second form of amyloid involved in AD pathophysiology. Similar to Aβ, circling amylin can aggregate to membrane-permeant toxic oligomers, diffuse into brain via blood-brain barrier (BBB) and accumulate to induce deleterious effects to brain involving inflammation, oxidative stress and neuronal dysregulation [20]. In addition, although amylin and Aβ have little similarities in their primary sequence, they share common secondary structures and biochemical features, such as commonalities as to deregulate the cellular proteome, impair mitochondrial functions

and neurocytotoxicity [21, 22]. Therefore, hyperamylinemia and amylin accumulation may be an important pathological mechanism linking diabetes with AD.

Increasing evidences show that amylin accumulation may induce oxidative stress by causing mitochondrial dysfunction [23]. Hyperamylinemia and amylin oligomerization increases the production of reactive oxygen species (ROS), decreases the level of endogenous antioxidant glutathione (GSH), and upregulates nitric oxide (NO) generation by reducing the activity of antioxidant enzymes, including superoxide dismutase (SOD), catalase (CAT) and glutathione peroxidase (GPx) [24-26], and by inducing the expression of nitric oxide synthase (iNOS) [27]. Amylin aggregates may be also a risk factor for cerebral inflammation, possibly by promoting the production of pro-inflammatory cytokines. These cytokines, specifically TNF-α and IL-1β, contribute to the feed-forward cycle by inducing further neuronal cell dysfunction and by forming more amylin and Aβ deposits[17, 28]. Hence, inhibiting amylin aggregation and cytotoxicity, reducing oxidative stress, and decreasing the production of NO and pro-inflammatory cytokines are rational therapeutics for treatment of diabetic brain injury and AD.

Flavonoids are a family of phenolic compounds with remarkable biochemical and pharmacological activities, such as antibacterial, antiviral, anti-inflammatory, anti-allergic, antithrombotic, antimutagenic, anti-neoplastic, and neuroprotective properties [29]. Rutin is a flavonoid found in various plants and foods that exhibits numerous pharmacological activities, such as free-radical scavenging, immune and inflammatory cell regulation, antioxidant and anti-inflammatory properties, and cytoprotective actions against aging and cancer [30]. Rutin prevents oxidative stress, mitochondrial dysfunction, and cell death in Caco-2 cells and has neuroprotective benefits in AD and Parkinson's diseases by mitigating cellular damage induced by ROS[31, 32]. Rutin may also decrease oxidative stress and the production of NO and pro-inflammatory cytokines induced by Aβ [33]. Moreover, our previous reports showed that rutin improved spatial memory in AD transgenic mice by reducing Aβ oligomer level and attenuating oxidative stress and neuroinflammation[34]. In addition, rutin has an anti-hyperglycemic and antioxidant effect on streptozotocin-induced diabetic Wistar rats [35]. Rutin analogs, such as quercetin, myricetin, morin hydrate,

4

oleuropeinaglycon, and silibinin, prevent amylin aggregation and disaggregate the formed amylin fibrils[36-40]. However, the effect of rutin on amylin-induced neurocytotoxicity and oxidative stress remains unclear. In this study, we will investigate the effect of rutin on amylin-induced neurotoxicity, oxidative stress, inflammatory reaction and nitric oxide (NO) generation in neuronal cells.

Results

Rutin attenuates amylin-mediated neurocytotoxicity and mitochondrial dysfunction

Similar to Aβ aggregation-induced AD pathology, amylin accumulation in the brain can injure the neuronal cells by forming membrane-permeant oligomers [24]. To test the effect of rutin on amylin-induced neurocytotoxicity, SH-SY5Y cells were incubated with amylin in the presence or absence of rutin and the cell viability was determined by MTT assay. Our results showed that the viability of cells treated with amylin (2 μM) alone remarkably decreased by 35.8%, whereas rutin improved cell viability in a concentration-dependent manner. Compared with amylin alone, 4 μM rutin) significantly inhibited amylin-induced cytotoxicity by approximately 54.5% ($P < 0.05$), and 4 μM rutin showed significant protective effects on neuronal cell viability than1 and 2 μM ($P < 0.05$) (Fig. 1A).

It is believed that amylin accumulation in the brain can lead to mitochondrial dysfunction [41], thus increasing cytotoxicity and inducing cell death. Hence we investigated the effect of rutin on amylin-induced mitochondrial dysfunction by mitochondrial membrane potential (MMP) assay. The fluorescent intensity ratio (red/green) of JC-1 in SH-SY5Y cells was decreased with the addition of amylin by 50%. However, 4 μM rutin drastically increased the ratio by 36%, and showed higher inhibitory effect than 2 and 1 μM (Fig. 1B). Our findings indicated that rutin can ameliorate amylin-induced mitochondrial dysfunction concentration-dependently.

Regulatory effect of rutin on MDA and SOD

MDA is an indicator of free radical-induced lipid peroxidation and serves as an oxidative stress marker[42]. To evaluate the effect of rutin on MDA production, the MDA level was determined in BV-2 cells pre-incubated with amylin in the presence or absence of rutin. The results showed that amylin

significantly increased MDA generation, whereas 0.8 and 8 μM rutin treatment markedly reduced amylin-induced MDA production by 49.7% and 56.7%, respectively ($P < 0.01$, Fig. 2A), which suggest rutin can protect neuronal cells from amylin-induced lipid peroxidation.

Oxidative stress has been strongly implicated in the pathophysiology of AD, which is closely related to the accumulation of Aβ and amylin in the brain [20]. SOD is a free radical scavenging enzyme and its activity is considered as another oxidative stress marker. To measure the effect of rutin on SOD activity，BV-2 cells were pre-incubated with amylin in the presence or absence rutin, and the SOD levels, including Total-SOD, Mn-SOD, and Cu/Zn-SOD levels were determined respectively. Our data demonstrated that all SOD levels markedly decreased with the addition of amylin, however, rutin restored these levels concentration dependently. Compared with amylin alone, both 0.8 μM and 8 μM rutin enhanced SOD levels, 8 μM rutin significantly increased Total-SOD, Mn-SOD, and Cu/Zn-SOD levels by 112% ($P < 0.01$), 133% ($P < 0.01$), and 96.8% ($P < 0.05$), respectively (Fig. 2B–D), while 0.8 μM rutin showed less beneficial effect than 8 μM. Moreover, the MDA/SOD ratio, an index of oxidative stress, was enhanced by amylin and reduced by rutin, which indicates that rutin attenuated amylin-induced lipid peroxidation and oxidative stress in neuronal cells (Fig. 2E).

Rutin reduces ROS production and increases CAT and GPx activity

ROS significantly affects many cellular pathological processes. Excessive ROS generation is a vital factor contribute to oxidative stress in AD development[42]. To determine the effect of rutin on amylin-induced ROS generation, SH-SY5Y cells were treated with 4 μM amylin in the absence or presence of rutin. The ROS levels were detected by using 2',7'-dichlorofluorescein diacetate (DCFH-DA). Our results showed that amylin significantly increased ROS production in SH-SY5Y cell cultures, while 0.8 μM and 8 μM rutin treatment noticeably inhibited amylin-induced ROS generation in a dose-dependent manner ($P < 0.05$, Fig. 3A).

Increased ROS can damage protein, lipid, and nucleic acids, reduce the activities of various antioxidant enzymes, such as CAT and GPx. Hence, we determined the activities of CAT and GPx in BV-2 cells treated with 4 µM amylin in the absence or presence of rutin. Our results showed that the activities of these antioxidant enzymes were decreased by amylin and restored by rutin. Relative to amylin alone, rutin (0.8 and 8 µM) increased CAT activity by approximately 23.3% and 43.6% ($P < 0.05$), and GPx activity by 64.7% and 115.2% ($P < 0.01$), respectively (Fig. 3B and C). Compared with 0.8 µM rutin, 8 µM rutin significantly enhanced the levels of CAT and GPx in BV-2 cells.

Regulatory effect of rutin on GSH and GSSG levels

GSH is a vital extracellular and intracellular protective antioxidant against oxidative stress. It reduces hydrogen peroxides and hydroperoxides by redox and detoxification reactions as well as protects protein thiol groups from oxidation. During detoxification and redox cycling, GPx converts GSH to GSSG in H_2O_2 catalysis to H_2O. GSSG can be converted back to GSH by glutathione reductase. Hence, GSH/GSSG ratio is an ideal indicator for oxidative stress level [43, 44]. The results demonstrated that amylin alone significantly decreased GSH levels and increased GSSG levels in BV-2 cells (Fig. 4A and B), while rutin addition markedly increased GSH (Fig. 4A) and decreased GSSG levels (Fig. 4B) in a concentration-dependent manner. Compared with 0.8 µM rutin, 8 µM rutin treatment significantly increased GSH levels and decreased GSSG levels. Consequently, the GSH/GSSG ratio was reduced by amylin and dose-dependently reinstated by rutin addition ($P < 0.01$, Fig. 4C).

Rutin reduces amylin-induced production of NO and iNOS

NO generated from iNOS is a key mediator of tissue damage after injury. Numerous evidences indicate that NO plays a pivotal role in the cascade of events leading to neuronal death. Moreover, Aβ can induce NO generation by upregulating the expression of iNOS [45]. Since amylin and Aβ share similar pathophysiology in AD development, we test the effect of rutin on amylin-induced NO and iNOS generation in SH-SY5Y cells by using 3-amino,4-aminomethyl-20,70-difluorescein diacetate (DAF-FM

DA). Our finding indicated that rutin (0.8 and 8 µM) significantly inhibited amylin-induced NO and iNOS generation ($P < 0.01$, Fig. 5A and B). Compared with 0.8 µM rutin, 8 µM rutin treatment significantly inhibited amylin-induced NO and iNOS generation.

Rutin reduces amylin-induced production of TNF-α and IL-β

Recently studies showed that amylin oligomers may promote cerebral inflammation, thus exacerbating BBB damage and further toxic brain amylin accumulation [20]. To assess the effect of rutin on the production of pro-inflammatory cytokines, TNF-α and IL-β levels was detected in the supernatants of BV-2 cells treated with amylin in the presence or absence of rutin. The results showed that both TNF-α and IL-β levels were increased by amylin addition while significantly decreased by rutin in a concentration-dependent manner (Fig. 6A and B). Compared with amylin alone, 8 µM rutin significantly decreased TNF-α and IL-β levels by 17.3% ($P < 0.05$) and 67.3% ($P < 0.01$), respectively. These findings suggested that rutin may exert anti-inflammatory effect by reducing pro-inflammatory cytokine generation.

Rutin inhibits amylin fibrillization

To investigate the mechanism by which rutin affects neuronal cells, the effect of rutin on amylin aggregation was determined. Similar to Aβ, amylin fibril generally forms via nucleation-dependent aggregation [46]. The kinetics of amylin fibril growth can be monitored by the specific binding of fluorescent molecule Thioflavin T (ThT) to amylin aggregates[47, 48]. Data demonstrated that up to 10 µM of amylin alone exhibited expected nucleation-dependent polymerization with a typical lag phase after incubation. Co-incubation with rutin significantly reduced the intensity of amylin fibril fluorescence, more than 50% and 95% fibril formation was inhibited by 100 and 300 µM of rutin, respectively (Fig. 7B). In addition, the morphology of the amylin fibrils was detected by transmission electron microscopy (TEM). Consistent with the ThT fluorescence results, 10 µM amylin alone formed and accumulated

abundant long fibers. The fibril formation was notably decreased with the addition of 100 µM rutin, and only a few short fibers were observed with 300 µM rutin (Fig. 7C–E).

Discussion

Amyloid proteins accumulation in tissues plays a critical role in the pathogenesis of various amyloidosis [4]. Currently increasing epidemiological studies establish a close association between T2DM and AD [21]. Recent research identified that extensive amylin accumulation and deposition were observed in the cerebral vasculature and brain parenchyma of patients with late onset AD. In the brain, amylin and Aβ may share common amyloidogenic features and similar pathogenic mechanisms. Amylin oligomers are believed to be the main toxic species and possibly form ion-permeable pores in lipid bilayer membranes, which disrupt ionic homeostasis across the cell membrane leading to neuronal cells damage and death [49]. Therefore, amylin oligomer may be a possible predictor of brain injury and dementia.

In our study, amylin exhibited significant cytotoxicity by markedly inhibiting SH-SY5Y cells viability in MTT assay, while flavonoid antioxidant rutin could remarkably attenuate this effect, which is consistent with our previous results of rutin's effect on Aβ-induced cytotoxicity [33]. The possible mechanism is small compound rutin may interact with amylin and modify the structure of amylin oligomers to inhibit cytotoxicity. Mitochondria are essential for ATP synthesis, Ca^{2+} homeostasis maintenance, redox signaling and antioxidant defence [50]. Due to the limited glycolytic capacity in neuronal cells, neurons rely heavily on ATP synthesis by mitochondria, and therefore, are particularly susceptible to disturbance in mitochondrial function [51]. Similar to Aβ, amylin oligomerization and deposition in the brain also leads to mitochondria dysfunction, our results indicated that rutin can protect SH-SY5Y cells from amylin-induced mitochondrial damage.

Oxidative stress is a potential contributor to the development of AD and T2DM, which occurs when free radical production exceeds antioxidant capacity. Overproduction of free radicals may cause an imbalance in the cell redox environment, induce lipid peroxidation, or attack proteins and nucleic acids to

cause metabolic dysfunction, ultimately leading to cell death [52]. Both amylin and Aβ accumulation in the brain are reported to induce brain injury by leading to oxidative stress and ROS formation, neuronal dysregulation and thus increasing neurocytotoxity [20]. The predominant source of ROS is mitochondrial oxidative phosphorylation. SOD combats ROS toxicity by catalytically reducing superoxide radical anions to hydrogen peroxide. CAT and GPx catalyze the transformation of hydrogen peroxide within the cell to harmless products, thereby curtailing the number of cells destroyed [53]. Therefore, scavenging free radicals and preventing lipid peroxidation can directly suppress oxidative damage. In current study, we revealed that amylin increased the ROS levels by inhibiting the anti-oxidative activity of SOD, CAT and GPx, while rutin, a flavonoid antioxidant abundant in daily food, enhances the status of endogenous antioxidant systems and protects neuronal cells from oxidative damage by inhibiting ROS production and increasing SOD, CAT and GPx activity [54].

Except for the antioxidant enzymes, decreased levels of non-enzymatic antioxidants such as GSH may induce oxidative stress. GSH homeostasis is maintained by GSH synthesis and redox cycling. During detoxification, oxy-radicals are reduced by GPx to form GSSG, while GSH is regenerated by redox recycling, whereby GSSG is reduced to GSH by glutathione reductase with the consumption of NADPH. In addition, free radicals attack polyunsaturated fatty acids inducing lipid peroxidation and lead to membrane damage and the production of MDA. Therefore, the oxidative stress level can also be evaluated by MDA, which is a key indicator for free radical-induced lipid peroxidation [54, 55]. In the present study, amylin induced oxidative stress by decreasing GSH levels and the GSH/GSSG ratio and raising MDA levels, whereas rutin exhibited antioxidant ability by increasing the GSH/GSSG ratio and downregulating the MDA levels. It has been reported that both the C-4 carbonyl group and the C-3 or C-5 hydroxyl group in the rutin structure may contribute to the antioxidant property by preventing the formation of free radicals in the Fenton system [56], indicating that rutin is a promising agent to block or delay AD and T2DM pathological progression.

10

Cerebral inflammation is considered a disruptor of normal synaptic function in AD development. NO production resulting from iNOS enzyme activation is a primary contributor to the inflammatory response. Although NO significantly affected host defense against various pathogens, the overproduction of NO can be harmful and result in various diseases[43, 54]. Therefore, therapeutic agents that inhibit iNOS activity may be useful in relieving inflammatory reactions. Our study showed that rutin reduced amylin-mediated NO production by decreasing iNOS activity. Similar to Aβ, amylin oligomer in AD brain may promote cerebral inflammation, probably by activating microglia cells to produce pro-inflammatory cytokines, such as TNF-α and IL-1β, which may trigger intracellular death-related signaling pathways to induce cell death thus leading to further toxic brain amylin accumulation in a feed-forward cycle [31]. In the present study, rutin effectively inhibited amylin-induced generation of TNF-α and IL-1β concentration dependently, which suggests that rutin may protect neuronal cells from amylin-induced deleterious effects by preventing pro-inflammatory cytokines production.

Amyloid aggregates significantly affect pathologic processes in various amyloidoses. Various of polyphenol compounds with an aromatic structure, such as quercetin and myricetin, have been reported to exhibit inhibitory effects on amylin aggregation and cytotoxicity [36, 37]. Thus we monitored amylin aggregation via ThT dyeing to test whether the benign effects of rutin are related to the inhibition of amylin assembly. Similar with Aβ, amylin typically aggregates via nucleation-dependent aggregation [12], but rutin inhibited amylin fibrillization (Fig. 7A–E). The mechanism underlying polyphenol compounds inhibit Aβ aggregation is that their aromatic structure can bind to Aβ hydrophobic β-sheet secondary structure and simultaneously disturb Aβ hydrogen bond formation through the action of hydroxyls as electron donors. Rutin, composed of an aromatic core with polyhydroxyl groups, may also exert the inhibitory effect on amylin aggregation through above mechanism.

Greater understanding of the mechanisms underlying the amylin oligomer-induced deleterious effects in the brain will potentially lead to new treatments. Reversing amylin-mediated brain injury by curbing cerebral amylin oligomer accumulation, inhibiting amylin oligomer-induced neurocytotoxicity and

oxidative stress may be therapeutic strategies to interfere AD development. In present study, rutin attenuates amylin cytotoxicity and prevents mitochondrial damage by inhibiting the generation of ROS, MDA, GSSG, NO, iNOS, and pro-inflammatory cytokines, and by increasing SOD, CAT and GPx activities, as well as GSH levels. These protective effects of rutin may partly result from the inhibition of amylin aggregation, which indicates that rutin has potential application in AD treatment.

Experimental

Materials

Amylin was purchased from the American Peptide Company (Sunnyvale, CA, USA). Rutin was provided by Dr. Dongling Niu of Ningxia University. The purity of rutin was analyzed by high-performance liquid chromatography (>95%). Rutin was dissolved in 100% dimethyl sulfoxide (DMSO) to 32 mM stock concentration and diluted with phosphate buffer saline (PBS, pH 7.4) to the indicated concentration. TNF-α and IL-1β ELISA kits were obtained from R&D Systems (Minneapolis, MN, USA). The assay kits for ROS, JC-1, MDA, GSH, GSSG, SOD, GPx, CAT, NO, and iNOS were purchased from Beyotime Company (Jiangsu, China).

MTT assay

Cell activity was measured by MTT assay as previously described[33]. SH-SY5Y neuroblastoma cells were maintained in Dulbecco's modified Eagle's medium (DMEM; Hyclone) with 10% fetal bovine serum (FBS) and 1% penicillin/streptomycin at 37 °C in 5% CO_2 atmosphere. The cells were seeded in 96-well plates with approximately 10,000 cells per 100 μL of medium per well. The plates were incubated for 24 h to allow the cells to attach at 37 °C. Then amylin was added with or without different concentrations of rutin. The final concentration of amylin was 2 μM. The plates were then incubated at 37 °C for another 48 h. Afterward, 10 μL of 5 mg/mL MTT was added to each well, the medium was gently removed after additional 3 h incubation, and 100 μL DMSO was added to each well. The plates were

shaken at 37 °C for 6 h to dissolve the crystals before the absorbance at 560 nm was measured by using a Tecan Safire 5 microplate reader (Switzerland). The averages from six replicate wells were used for each sample and the control. Each experiment was conducted three times.

MMP assay

JC-1(5,5',6,6'-tetrachloro-1,1',3,3'-tetraethylbenzimidazolylcarbocyanine iodide) was used as a fluorescent probe to test MMP in SH-SY5Y cells. In normal cells, JC-1 exists as a monomer (green) in the cytosol and accumulates as aggregates (red) in the mitochondria through the induction of higher MMP. In apoptotic and necrotic cells, JC-1 remains in monomeric form and stains the cytosol green. SH-SY5Y cells cultured in 96-well plates were treated with amylin and rutin as above and then incubated with JC-1 staining solution (5 μg/mL) at 37 °C for 20 min. The fluorescence intensity of both mitochondrial JC-1 monomers (λex 514 nm and λem 529 nm) and aggregates (λex 585 nm and λem 590 nm) were detected by using the Tecan Safire 5 microplate reader. The $\Delta \Psi m$ of the cells was calculated as the fluorescence ratio of red to green.

ROS assay

ROS production was fluorometrically monitored by using DCFH-DA in SH-SY5Y cell cultures[57]. The cells were treated with 4 μM amylin or a mixture of 4 μM amylin with 0.8 or 8.0 μM rutin and incubated at 37 °C overnight in 96-well plates. After the cells were washed three times with PBS, DCFH-DA was diluted in fresh phenol red-free DMEM to a final concentration of 5 μM and incubated with the cells at 37 °C for 20 min. The chemicals were then removed and the cells were washed three times. Relative ROS units were determined by using the Tecan Safire 5 microplate reader (λex 485 nm and λem 530 nm). ROS production was expressed as a percentage of the control.

Measurement of MDA, GSH, and GSSG

13

MDA concentration was determined by the thiobarbituric acid (TBA) test as previously described [58]. MDA reacts with TBA to form MDA-(TBA)2, a red adduct with maximum absorbance at 532 nm. Total GSH (T-GSH) was assayed by 5,5-dithio-bis (2-nitrobenzoic) acid (DTNB)–GSSG reductase recycling. GSSG was obtained by measuring the absorbance of 5-thio-2-nitrobenzoic acid (TNB) which was produced from the reaction of reduced GSH with DTNB according to the kit protocols.

BV-2 microglial cells were maintained in DMEM with 10% FBS and 1% penicillin/streptomycin at 37 °C in 5% CO_2. The cells were treated with or without 0.8 or 8.0 μM rutin for 30 min before the addition of 4 μM amylin, and then incubated at 37 °C overnight. Then the cells were collected and cell lysates were obtained by centrifuging at 10,000×g for 15 min at 4 °C. For the MDA measurement, the cell lysates were added to the detection solution of MDA, boiled for 15 min and followed by centrifugation at 1000×g for 10 min. Then the supernatant was used to test the relative MDA units through the Tecan Safire 5 microplate reader (532 nm). GSH and GSSG in the supernatant were also determined by using the Tecan Safire 5 microplate reader (412 nm) after incubation with the detection solution for 25 min at room temperature.

Measurement of SOD

Total SOD (T-SOD) and Mn-SOD activities in BV-2 microglial cells were detected by using SOD assay kits according to the manufacturer's protocols[59]. Briefly, the cells were treated as above. Then cell lysates were mixed with nitroblue tetrazolium (NBT) and enzyme working solutions and incubated at 37 °C for 20 min, the absorbance was recorded at 560 nm by using the Tecan Safire 5 microplate reader. Cu and Zn-SOD activities were measured by subtracting Mn-SOD activity from T-SOD activity.

Measurement of GPx and CAT

GPx activity in the supernatant of BV-2 microglial cell lysates was determined according to the kit protocol[60]. In brief, the samples were mixed with the GPx detection working solution (10 mM NADPH,

84 mM GSH, glutathione reductase, and 15 mM t-Bu-OOH), and the absorbance was measured immediately at 340 nm and monitored every 30 s for 3 min at 25 °C. One unit was defined as the amount of enzyme that oxidized 1 μM of NADPH to $NADP^+$ per min at 25 °C.

CAT activity was analyzed as previously described[61]. The samples were treated with excess hydrogen peroxide and incubated for 5 min. Then the hydrogen peroxide which was not decomposed by CAT was coupled with a substrate to produce N-4-antipyryl-3-chloro-5-sulfonate-p-benzoquinonemonoimine by peroxidase treatment, which has an absorption maximum of 520 nm. The CAT unit was defined as the amount of enzyme that catalyzed 1 μM of H_2O_2 to H_2O and O_2 per min at 25 °C.

Measurement of NO and iNOS

NO production in SH-SY5Y cells was fluorometrically monitored by using 3-amino,4-aminomethyl-20,70-difluorescein, diacetate (DAF-FM DA) as previously described [62]. The cells were pretreated with rutin for 30 min prior to the addition of 4 μM amylin and incubated at 37 °C for 12 h. Then DAF-FM DA (5 μM) was added to the cells and incubated at 37 °C for additional 20 min. The chemicals were then removed and the cells were washed three times with PBS. The fluorescence intensity was determined by using the Tecan Safire 5 microplate reader (λex 495 nm and λem 515 nm). NO production was expressed as a percentage of the control.

Total NOS (T-NOS) and non-iNOS activities were detected according to the kit protocol. iNOS activity was calculated by subtracting non-iNOS activity from T-NOS activity. Briefly, SH-SY5Y cells were treated with amylin in the presence or absence rutin as above. The culture supernatant was removed and 100 μl of NOS assay buffer (1×) or iNOS inhibitor (1 mM L-canavanine sulfate salt) was added to the wells for NOS and non-iNOS detection, respectively. Then, 100 μl of NOS assay reaction solution (50% NOS assay buffer, 39.8% water, 5% L-arginine solution, 5% 0.1 mM nicotinamide adenine dinucleotide phosphate [NADPH], 0.2% DAF-FM DA) was added to each well and incubated for 30 min

at 37 °C. Fluorescence was measured by using the Tecan Safire 5 microplate reader (λex 495 nm and λem

515 nm).

Measurement of TNF-α and IL-β

BV-2 microglial cells were incubated with 4 μM amylin with or without rutin for 12 h, then the cell

supernatants were collected, and the levels of TNF-α and IL-1β released from activated BV-2 cells were

determined by using the TNF-α and IL-1β ELISA kits according to the manufacturer's protocols.

Preparation of amylin aggregates

Amylin was dissolved in 100% 1,1,1,3,3,3-hexafluoro-2-propanol (HFIP) to a concentration of 1

mg/mL, sonicated in a water bath for 5 min, then aliquoted into Eppendorf tubes, dried in vacuum and

stored at −20 °C. Immediately before use, the HFIP-treated amylin was dissolved in DMSO to 2 mg/mL,

diluted to 10 μM in PBS (pH 7.4), and incubated at 37 °C without shaking to aggregate.

ThT fluorescence assay

To determine amyloid fibril formation, 10 μl of the incubated amylin with or without rutin was

periodically added to 190 μl of 5 μM ThT in 50 mM PBS (pH 6.5) in a 96-well black plate. Fluorescence

was measured by the Tecan Safire 5 microplate reader with excitation at 450 nm and emission at 482 nm.

Each reading represented the average of three values determined by a time scan after subtracting the

fluorescence contribution from the control solution. Each assay was performed in triplicate.

TEM imaging

TEM was used to observe the effect of rutin on amylin fibril formation[63]. Amylin monomers were

incubated at 37 °C with or without rutin for the indicated time, and then spotted onto a glow-discharged,

formvar-coated copper grid (Electron Microscopy Sciences, Hatfield, PA, USA) for 20 min. The sample

was displaced with an equal volume of 2.5% (v/v) glutaraldehyde in water for 5 min. Finally, the grid was

stained twice with 10 µL of 2% (v/v) filtered (0.2 mm) uranyl acetate in water for 30 s and allowed to dry

at room temperature. The samples were examined by a Hitachi H7650 TEM at 80 kV (Hitachi, Japan)

with a 5000× magnification.

Statistical analysis

The data were obtained from at least three separate experiments for each experimental condition and

presented as mean ± standard deviation, and their statistical significance was analyzed by Student's t test

or one-way ANOVA followed by Tukey's multiple comparison test.

Acknowledgments

References

1. R. Gupta, N. Kapoor, D. P. Raleigh and T. P. Sakmar, *Journal of molecular biology*, 2012, **421**, 378-389.

2. S. Chen, F. A. Ferrone and R. Wetzel, *Proc Natl Acad Sci U S A*, 2002, **99**, 11884-11889.

3. D. J. Selkoe, *Nat Cell Biol*, 2004, **6**, 1054-1061.

4. F. Chiti and C. M. Dobson, *Annual review of biochemistry*, 2006, **75**, 333-366.

5. L. Marzban, K. Park and C. B. Verchere, *Exp Gerontol*, 2003, **38**, 347-351.

6. A. Clark and M. R. Nilsson, *Diabetologia*, 2004, **47**, 157-169.

7. E. T. Jaikaran and A. Clark, *Biochim Biophys Acta*, 2001, **1537**, 179-203.

8. S. E. Kahn, D. A. D'Alessio, M. W. Schwartz, W. Y. Fujimoto, J. W. Ensinck, G. J. Taborsky, Jr. and D. Porte, Jr., *Diabetes*, 1990, **39**, 634-638.

9. A. Clark, G. J. Cooper, C. E. Lewis, J. F. Morris, A. C. Willis, K. B. Reid and R. C. Turner, *Lancet*, 1987, **2**, 231-234.

10. S. Bedrood, Y. Li, J. M. Isas, B. G. Hegde, U. Baxa, I. S. Haworth and R. Langen, *The Journal of biological chemistry*, 2012, **287**, 5235-5241.

11. J. Zhao, Y. Luo, H. Jang, X. Yu, G. Wei, R. Nussinov and J. Zheng, *Biochim Biophys Acta*, 2012, **1818**, 3121-3130.

12. L. Khemtemourian, J. A. Killian, J. W. Hoppener and M. F. Engel, *Exp Diabetes Res*, 2008, **2008**, 421287.

13. B. Konarkowska, J. F. Aitken, J. Kistler, S. Zhang and G. J. Cooper, *FEBS J*, 2006, **273**, 3614-3624.

14. Y. Li, M. M. Hatmal, R. Langen and I. S. Haworth, *J Chem Inf Model*, 2012, **52**, 2983-2991.

15. S. A. Jayasinghe and R. Langen, *The Journal of biological chemistry*, 2004, **279**, 48420-48425.

16. K. Jackson, G. A. Barisone, E. Diaz, L. W. Jin, C. DeCarli and F. Despa, *Annals of neurology*, 2013, **74**, 517-526.

17. G. S. Desai, C. Zheng, T. Geetha, S. T. Mathews, B. D. White, K. W. Huggins, C. A. Zizza, T. L. Broderick and J. R. Babu, *Journal of Alzheimer's disease : JAD*, 2014, **42**, 347-356.

18. J. A. Luchsinger, M. X. Tang, Y. Stern, S. Shea and R. Mayeux, *American journal of epidemiology*, 2001, **154**, 635-641.

19. L. Li and C. Holscher, *Brain research reviews*, 2007, **56**, 384-402.

20.   F. Despa and C. Decarli, *Expert review of proteomics*, 2013, **10**, 403-405.

21.   J. Gotz, Y. A. Lim and A. Eckert, *Frontiers in aging neuroscience*, 2013, **5**, 38.

22.   Y. A. Lim, L. M. Ittner, Y. L. Lim and J. Gotz, *FEBS letters*, 2008, **582**, 2188-2194.

23.   Y. Yang and W. Song, *Neuroscience*, 2013, **250**, 140-150.

24.   P. Westermark, A. Andersson and G. T. Westermark, *Physiol Rev*, 2011, **91**, 795-826.

25.   J. Montane, A. Klimek-Abercrombie, K. J. Potter, C. Westwell-Roper and C. Bruce Verchere, *Diabetes Obes Metab*, 2012, **14 Suppl 3**, 68-77.

26.   R. P. Robertson, J. Harmon, P. O. Tran and V. Poitout, *Diabetes*, 2004, **53 Suppl 1**, S119-124.

27.   U. Zumsteg, S. Frigerio and G. A. Hollander, *Diabetes*, 2000, **49**, 39-47.

28.   C. Westwell-Roper, D. L. Dai, G. Soukhatcheva, K. J. Potter, N. van Rooijen, J. A. Ehses and C. B. Verchere, *J Immunol*, 2011, **187**, 2755-2765.

29.   W. Arjumand, A. Seth and S. Sultana, *Food Chem Toxicol*, 2011, **49**, 2013-2021.

30.   J. Pyrzanowska, A. Piechal, K. Blecharz-Klin, I. Joniec-Maciejak, A. Zobel and E. Widy-Tyszkiewicz, *Pharmacol Rep*, 2012, **64**, 808-816.

31.   M. M. Khan, S. S. Raza, H. Javed, A. Ahmad, A. Khan, F. Islam, M. M. Safhi and F. Islam, *Neurotox Res*, 2012, **22**, 1-15.

32.   C. Carrasco-Pozo, M. L. Mizgier, H. Speisky and M. Gotteland, *Chem Biol Interact*, 2012, **195**, 199-205.

33.   S. W. Wang, Y. J. Wang, Y. J. Su, W. W. Zhou, S. G. Yang, R. Zhang, M. Zhao, Y. N. Li, Z. P. Zhang, D. W. Zhan and R. T. Liu, *Neurotoxicology*, 2012, **33**, 482-490.

34.   P. X. Xu, S. W. Wang, X. L. Yu, Y. J. Su, T. Wang, W. W. Zhou, H. Zhang, Y. J. Wang and R. T. Liu, *Behavioural brain research*, 2014, **264**, 173-180.

35.   N. Kamalakkannan and P. S. Prince, *Basic Clin Pharmacol Toxicol*, 2006, **98**, 97-103.

36.   K. Jimenez-Aliaga, P. Bermejo-Bescos, J. Benedi and S. Martin-Aragon, *Life Sci*, 2011, **89**, 939-945.

37.   C. Zelus, A. Fox, A. Calciano, B. S. Faridian, L. A. Nogaj and D. A. Moffet, *Open Biochem J*, 2012, **6**, 66-70.

38.   H. Noor, P. Cao and D. P. Raleigh, *Protein Sci*, 2012, **21**, 373-382.

39.   B. Cheng, H. Gong, X. Li, Y. Sun, X. Zhang, H. Chen, X. Liu, L. Zheng and K. Huang, *Biochem Biophys Res Commun*, 2012, **419**, 495-499.

40. S. Rigacci, V. Guidotti, M. Bucciantini, M. Parri, C. Nediani, E. Cerbai, M. Stefani and A. Berti, *J Nutr Biochem*, 2010, **21**, 726-735.

41. Y. A. Lim, V. Rhein, G. Baysang, F. Meier, A. Poljak, M. J. Raftery, M. Guilhaus, L. M. Ittner, A. Eckert and J. Gotz, *Proteomics*, 2010, **10**, 1621-1633.

42. K. Schuessel, C. Frey, C. Jourdan, U. Keil, C. C. Weber, F. Muller-Spahn, W. E. Muller and A. Eckert, *Free radical biology & medicine*, 2006, **40**, 850-862.

43. H. Javed, M. M. Khan, A. Ahmad, K. Vaibhav, M. E. Ahmad, A. Khan, M. Ashafaq, F. Islam, M. S. Siddiqui, M. M. Safhi and F. Islam, *Neuroscience*, 2012, **210**, 340-352.

44. R. A. Khan, M. R. Khan and S. Sahreen, *BMC Complement Altern Med*, 2012, **12**, 178.

45. Q. Wang, M. J. Rowan and R. Anwyl, *The Journal of neuroscience : the official journal of the Society for Neuroscience*, 2004, **24**, 6049-6056.

46. S. B. Padrick and A. D. Miranker, *Biochemistry*, 2002, **41**, 4694-4703.

47. J. D. Harper and P. T. Lansbury, Jr., *Annual review of biochemistry*, 1997, **66**, 385-407.

48. H. Naiki, K. Higuchi, M. Hosokawa and T. Takeda, *Anal Biochem*, 1989, **177**, 244-249.

49. M. Anguiano, R. J. Nowak and P. T. Lansbury, Jr., *Biochemistry*, 2002, **41**, 11338-11343.

50. M. P. Mattson, M. Gleichmann and A. Cheng, *Neuron*, 2008, **60**, 748-766.

51. X. J. Han, K. Tomizawa, A. Fujimura, I. Ohmori, T. Nishiki, M. Matsushita and H. Matsui, *Acta medica Okayama*, 2011, **65**, 1-10.

52. R. A. Khan, M. R. Khan and S. Sahreen, *BMC Complement Altern Med*, 2012, **12**, 204.

53. N. Kamalakkannan and P. Stanely Mainzen Prince, *Mol Cell Biochem*, 2006, **293**, 211-219.

54. Y. C. Yang, H. Y. Lin, K. Y. Su, C. H. Chen, Y. L. Yu, C. C. Lin, S. L. Yu, H. Y. Yan, K. J. Su and Y. L. Chen, *Evid Based Complement Alternat Med*, 2012, **2012**, 980276.

55. E. Moretti, L. Mazzi, G. Terzuoli, C. Bonechi, F. Iacoponi, S. Martini, C. Rossi and G. Collodel, *Reprod Toxicol*, 2012, **34**, 651-657.

56. P. Stanley Mainzen Prince and N. Kamalakkannan, *J Biochem Mol Toxicol*, 2006, **20**, 96-102.

57. S. G. Yang, W. Y. Wang, T. J. Ling, Y. Feng, X. T. Du, X. Zhang, X. X. Sun, M. Zhao, D. Xue, Y. Yang and R. T. Liu, *Neurochemistry international*, 2010, **57**, 914-922.

58. C. C. Winterbourn and I. H. Buss, *Methods in enzymology*, 1999, **300**, 106-111.

59. L. Sun, C. Guo, D. Liu, Y. Zhao, Y. Zhang, Z. Song, H. Han, D. Chen and Y. Zhao, *Neuroscience*, 2011, **184**, 151-163.

60. S. Rattanajarasroj and S. Unchern, *Neurochemical research*, 2010, **35**, 1196-1205.

61. Z. He, S. Yu, G. Mei, M. Zheng, M. Wang, Y. Dai, B. Tang and N. Li, *Free radical biology & medicine*, 2008, **45**, 1135-1142.

62. N. Nakatsubo, H. Kojima, K. Kikuchi, H. Nagoshi, Y. Hirata, D. Maeda, Y. Imai, T. Irimura and T. Nagano, *FEBS letters*, 1998, **427**, 263-266.

63. Y. Feng, X. P. Wang, S. G. Yang, Y. J. Wang, X. Zhang, X. T. Du, X. X. Sun, M. Zhao, L. Huang and R. T. Liu, *Neurotoxicology*, 2009, **30**, 986-995.
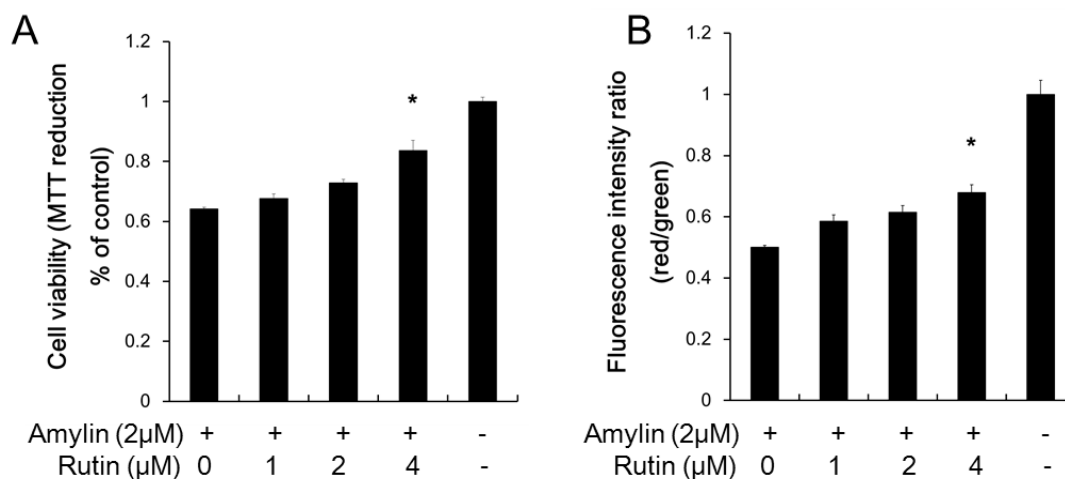
Fig. 1 Effect of rutin on amylin-induced cytotoxicity and mitochondrial membrane potential. (A) Amylin mixed with or without rutin was added to SH-SY5Y cells and incubated for 48h at 37 °C. Then the cell viability was detected by MTT assays. The absorbance was measured at 560 nm. Data was expressed as the percentage of control values from three independent experiments, with each experimental value being the average of six replicate wells. (B) Mitochondrial membrane potential was measured by using potential-sensing fluorescent probe (JC-1) in SH-SY5Y cells treated with 2 μM amylin in the presence or absence of rutin. The fluorescence intensity of both mitochondrial JC-1 monomers (λex 514 nm, λem 529 nm) and aggregates (λex 585 nm, λem 590 nm) were measured. The Δψm of SH-SY5Y cells was calculated as the fluorescence ratio of red to green (compared with amylin alone, *, $P < 0.05$).
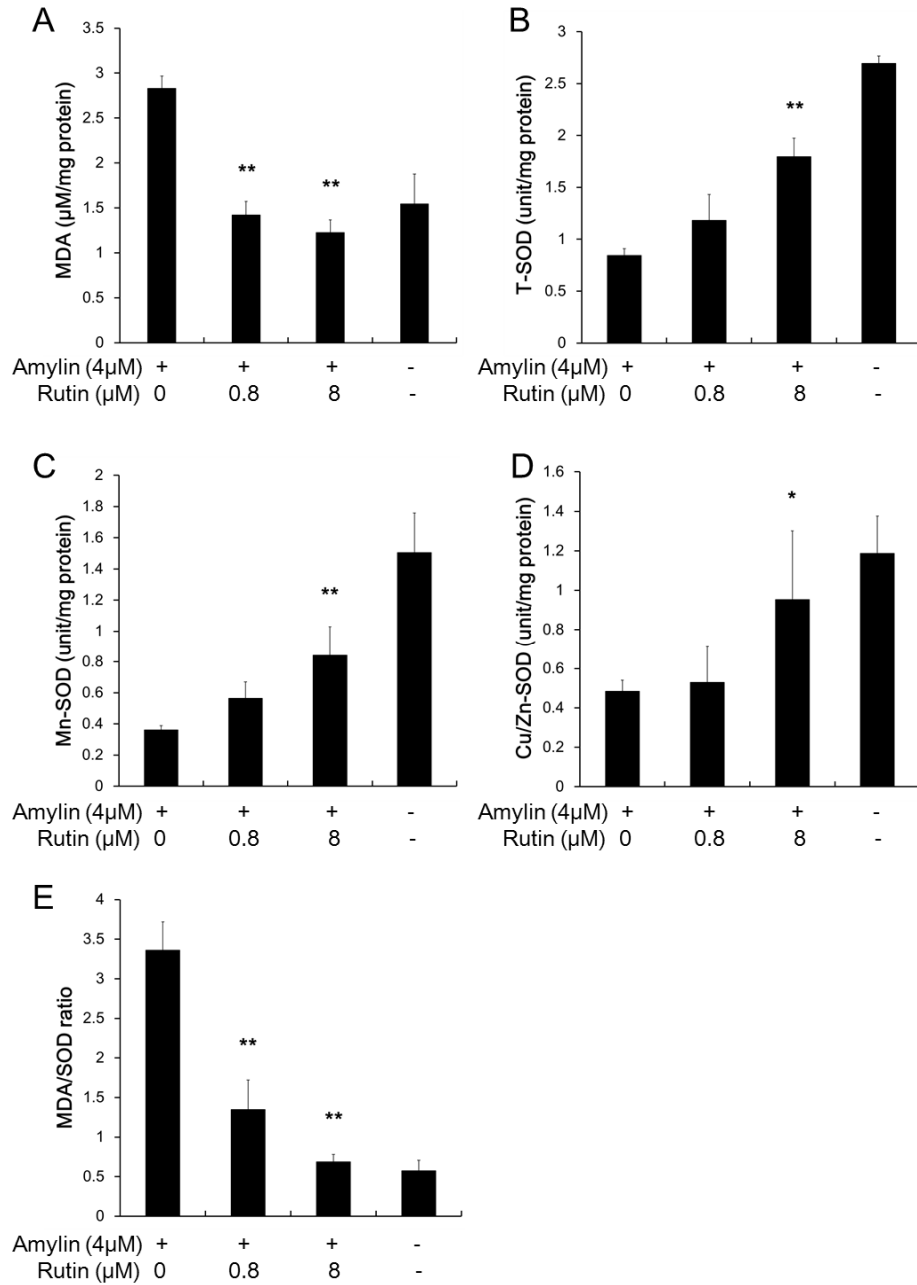
Fig. 2 Effect of rutin on MDA level and SOD activity. BV-2 cells were treated with 4 μM amylin in the presence or absence of 0.8 μM or 8 μM rutin and then incubated for 12 h. The level of MDA (A) was measured at 532 nm, and Total-SOD (B) and Mn-SOD (C) activities were measured at 560nm. Cu, Zn-SOD (D) and MDA/SOD ratio (E) was calculated (compared with amylin alone, *, $P < 0.05$, **, $P<0.01$).
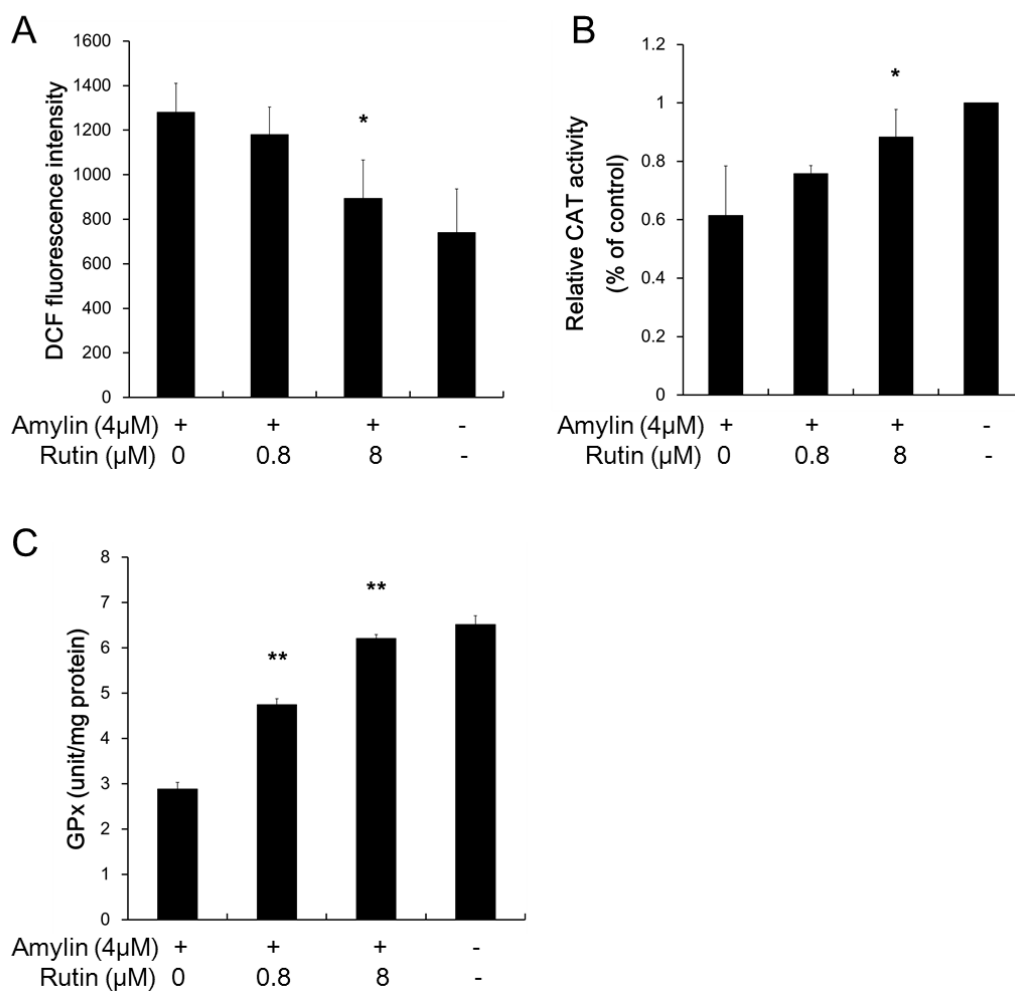
Fig. 3 Effect of rutin on amylin-induced ROS production and activities of CAT and GPx. (A) The ROS level was fluorometrically measured by using DCFH-DA dye in SH-SY5Y cells pre-treated with amylin in the presence or absence of rutin. The activities of CAT (B) and GPx (C) were determined in BV-2 cells incubated with 4 μM amylin with or without rutin (compared with amylin alone, *, $P < 0.05$, **, $P<0.01$).
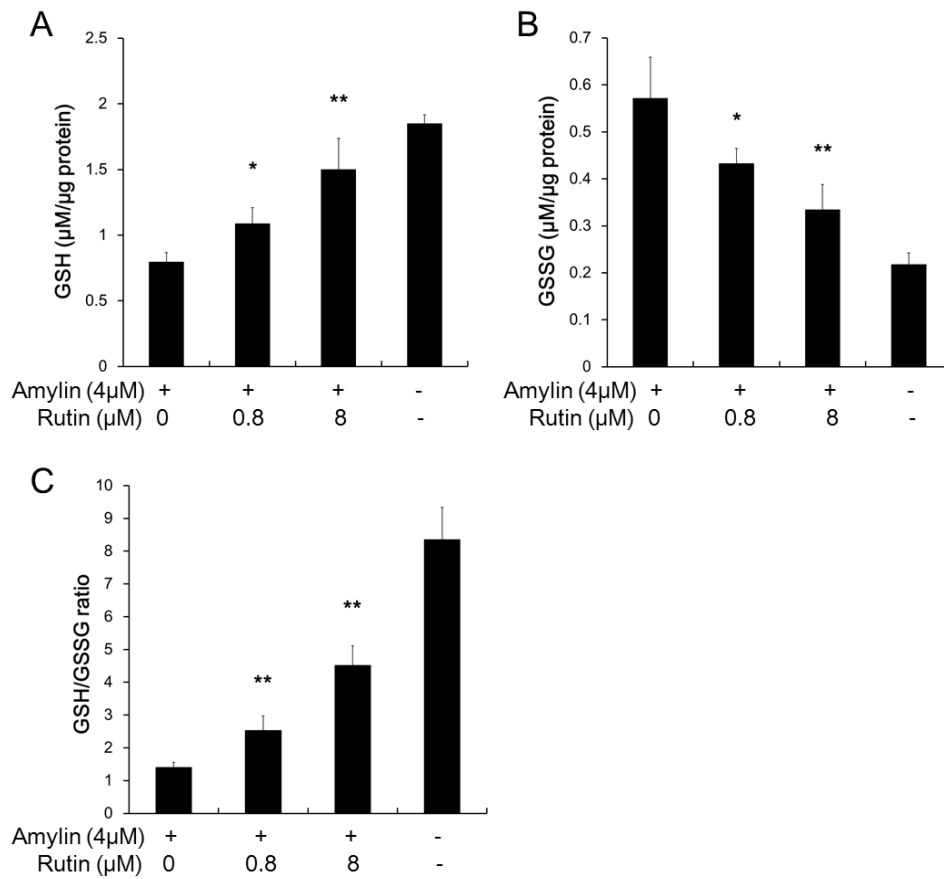
Fig. 4 Effect of rutin on amylin-induced GSH and GSSG levels. BV-2 cells were treated with amylin in the presence or absence of 0.8 or 8 μM rutin for 12 h. The level of GSH (A) and GSSG (B) was determined using a DNTB method and the GSH/GSSG ratio (C) was calculated (compared with amylin alone, *, $P < 0.05$, **, $P<0.01$).
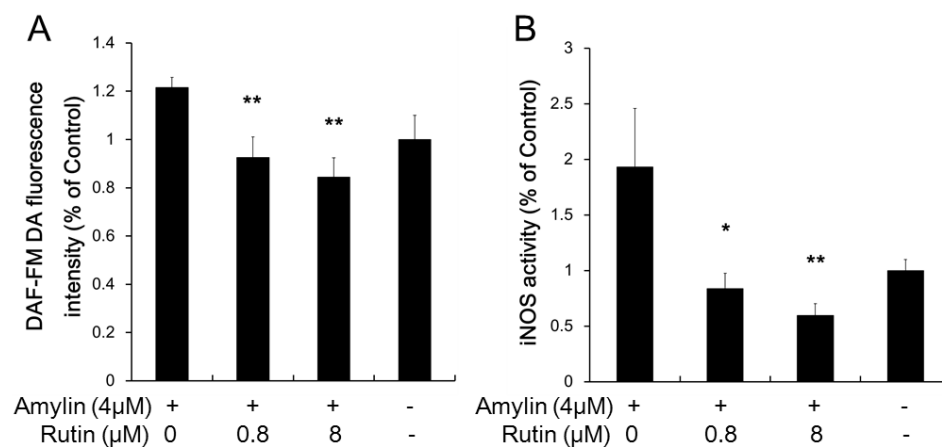
Fig. 5 Effect of rutin on amylin-induced NO production and iNOS activity. SH-SY5Y cells were pretreated with 0.8 or 8 μM of rutin for 30 min and then co-incubated with 4 μM amylin for 12 h. NO levels (A) and iNOS activity (B) were detected by measuring the fluorescence intensity of DAF-FM DA (λex 495 nm, λem 515 nm) using Tecan Safire 5 microplate reader (compared with amylin alone, *, $P < 0.05$, **, $P < 0.01$).
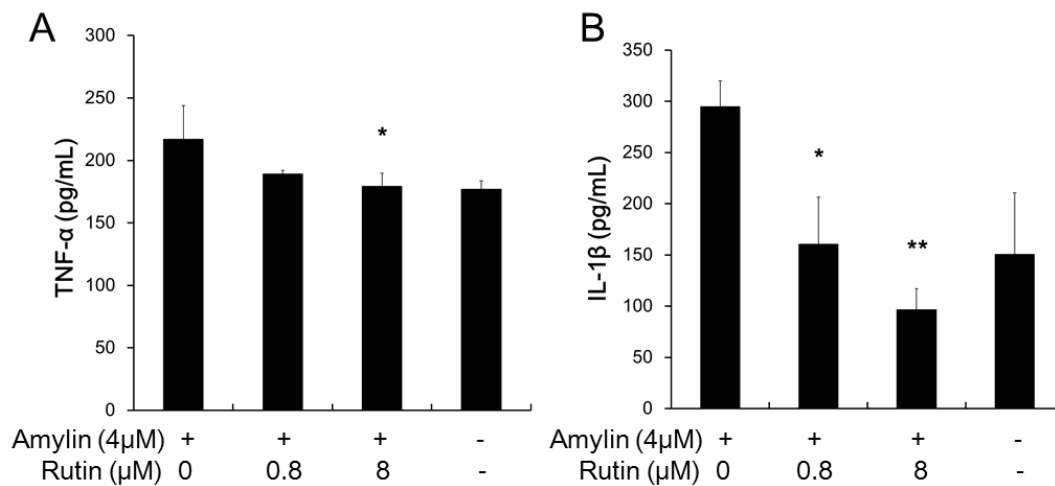
Fig. 6 Effect of rutin on the production of TNF-α and IL-1β. BV-2 cells were pretreated with 0.8 or 8 μM

of rutin for 30 min and then co-incubated with 4 μM amylin for 12 h. The supernatants were collected and

the levels of TNF-α (A) and IL-1β (B) were determined using ELISA kits (compared with amylin alone,

*, $P < 0.05$, **, $P < 0.01$).
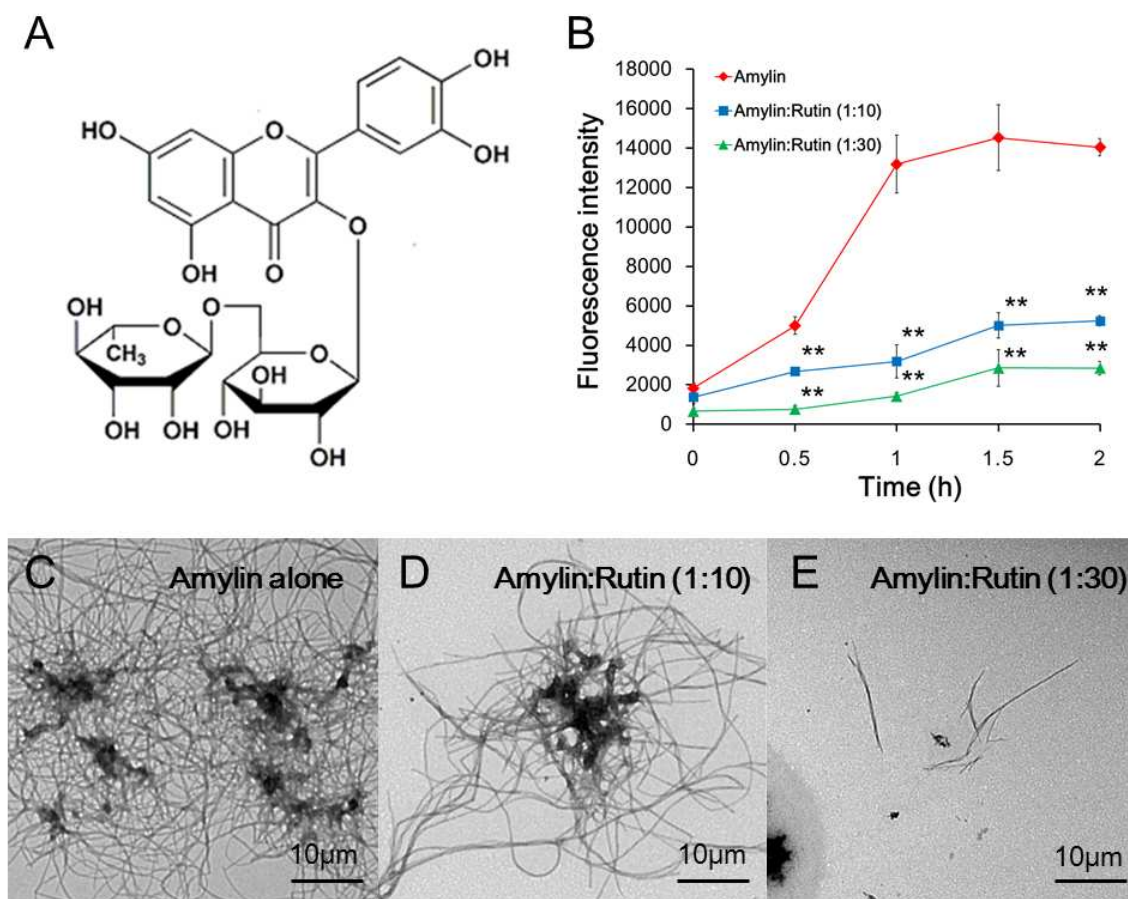
Fig. 7 Effect of rutin on the aggregation of amylin. (A) The chemical structure of rutin. (B) Amylin (10 μM) aggregation was monitored by ThT fluorescence in the presence or absence of 100 and 300 μM rutin. Fluorescence intensity was measured at an excitation wavelength of 450 nm and an emission wavelength of 482 nm (compared with amylin alone, **, $P<0.01$). The morphologies of amylin alone (C), and amylin incubated with 100 μM (D) and 300 μM rutin (E) were determined by a Hitachi H7650 TEM at 80 kV.

28
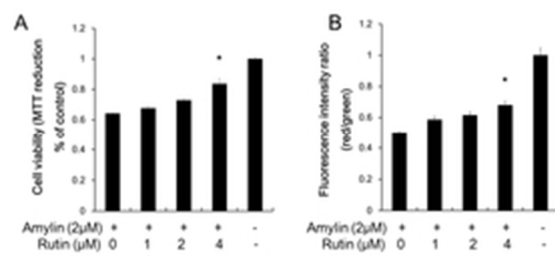
12x5mm (600 x 600 DPI)

37x53mm (600 x 600 DPI)

A

DCF fluorescence intensity

| Amylin (4µM) | + | + | + | - |
| Rutin (µM) | 0 | 0.8 | 8 | - |

B

Relative CAT activity (% of control)

| Amylin (4µM) | + | + | + | - |
| Rutin (µM) | 0 | 0.8 | 8 | - |

C

GPx (unit/mg protein)

| Amylin (4µM) | + | + | + | - |
| Rutin (µM) | 0 | 0.8 | 8 | - |
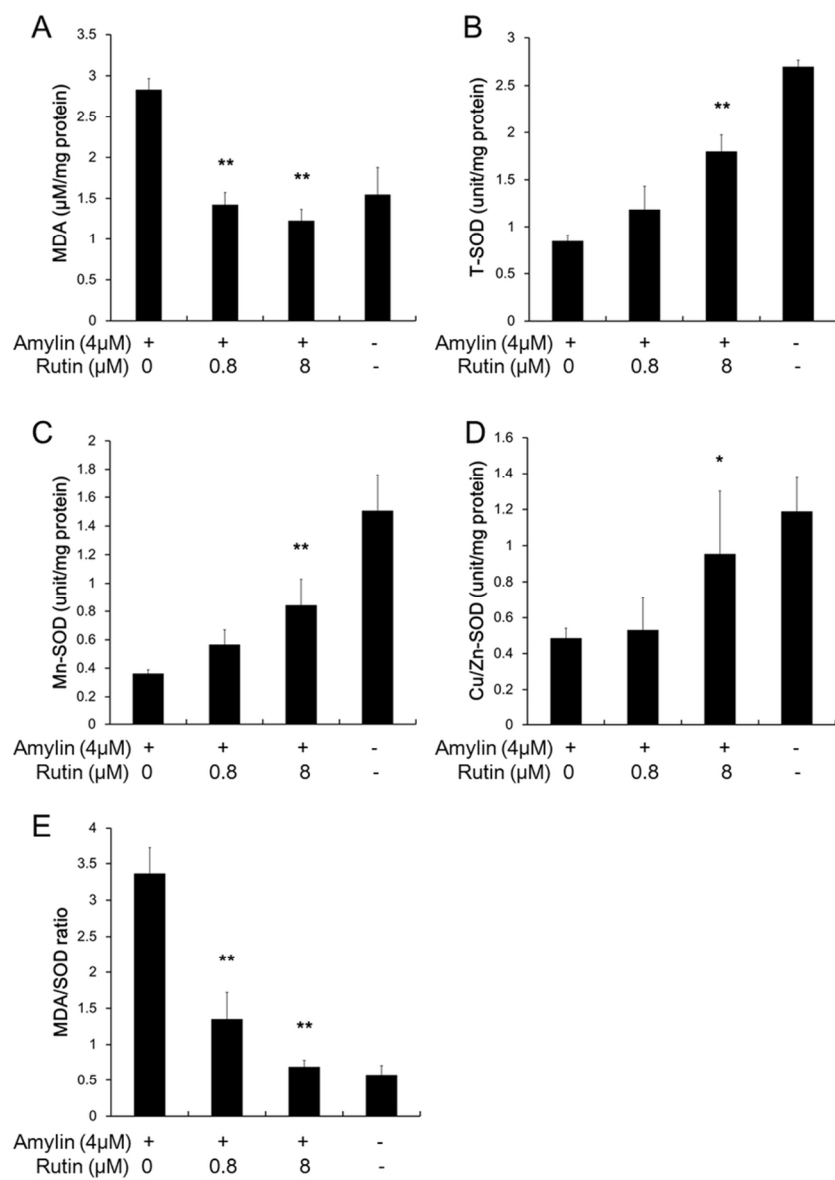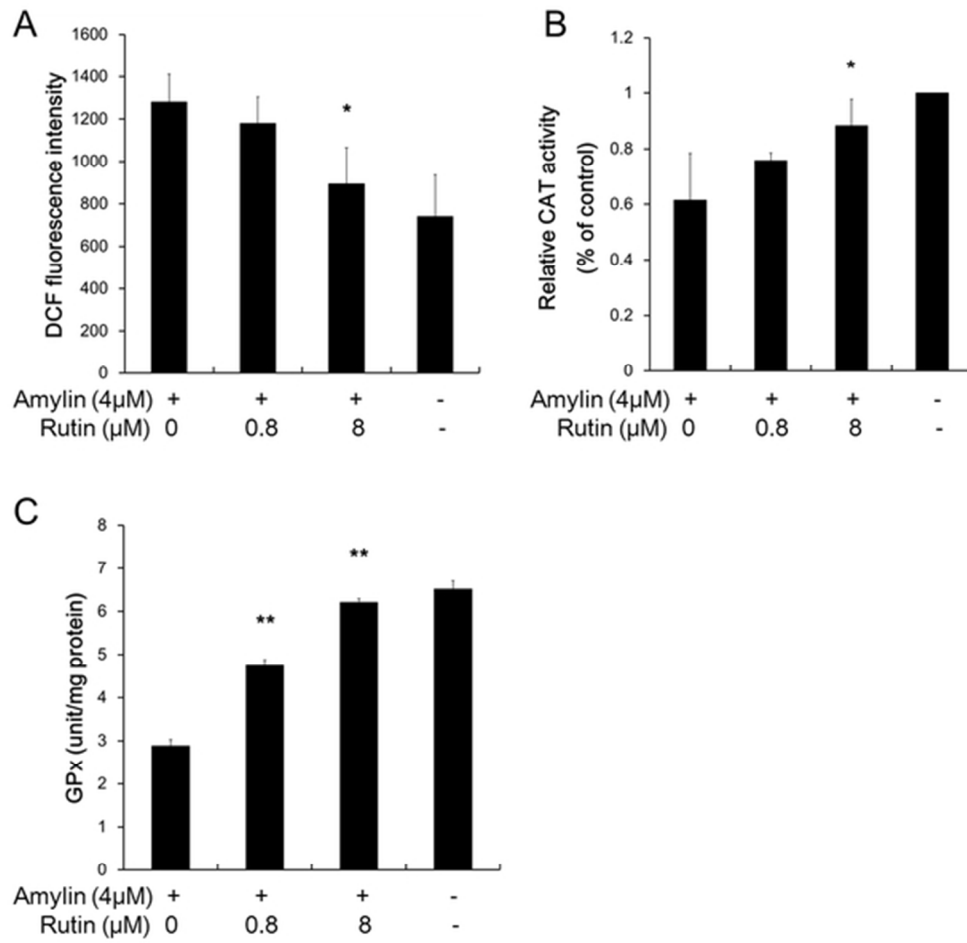
26x26mm (600 x 600 DPI)
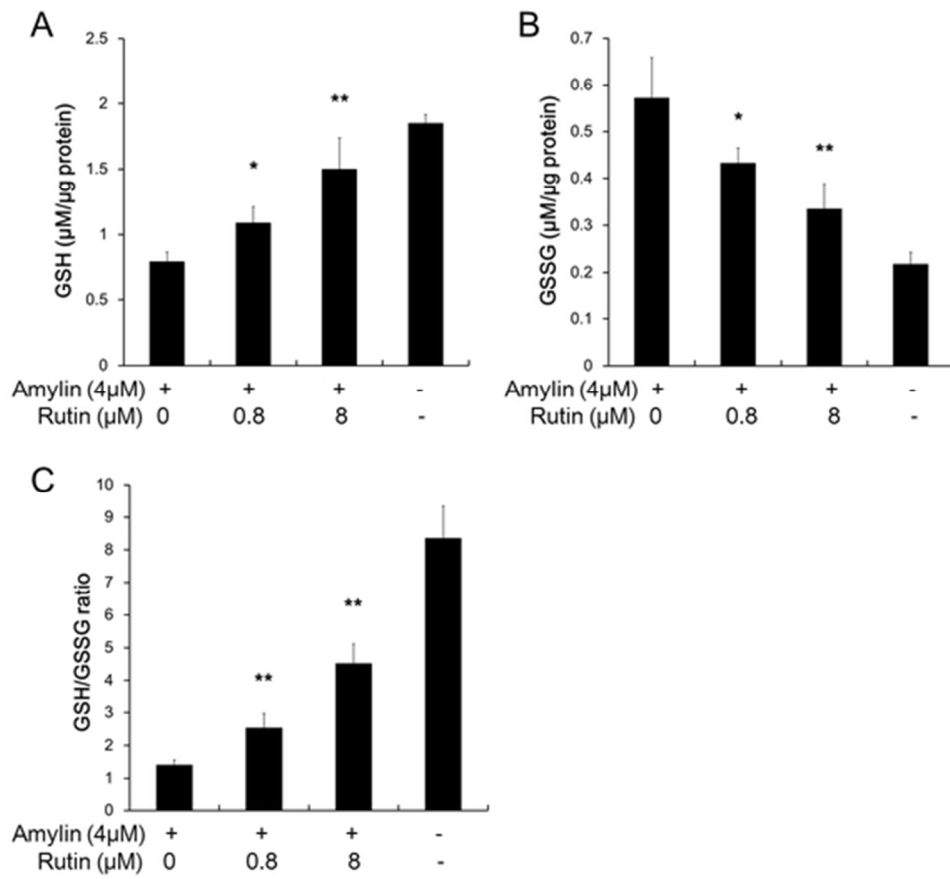
25x23mm (600 x 600 DPI)
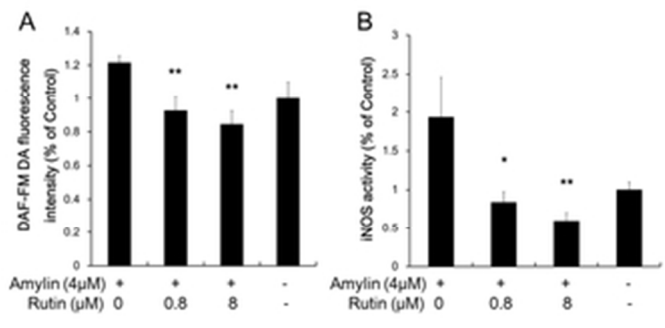
15x8mm (600 x 600 DPI)
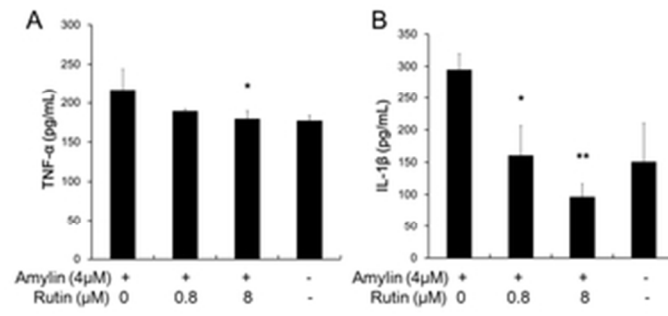
15x8mm (600 x 600 DPI)
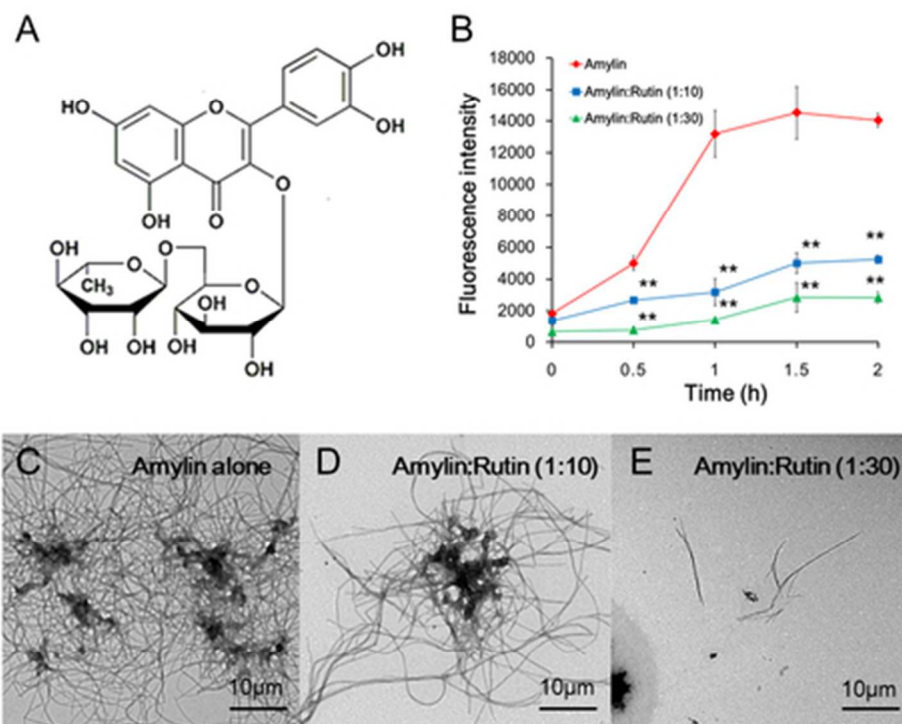
20x16mm (600 x 600 DPI)

Rutin inhibited amylin aggregation, amylin-induced neurocytotoxicity, and decreased the production of ROS, NO, GSSG, malondialdehyde and pro-inflammatory cytokines